European Journal of Medicinal Chemistry 141 (2017) 169–177

Contents lists available at ScienceDirect

European Journal of Medicinal Chemistry

journal homepage: http://www.elsevier.com/locate/ejmech

Research paper

Fragment-based approach to identify IDO1 inhibitor building blocks

Alice Coletti [a, 1], Francesca Camponeschi [b, 1], Elisa Albini [d], Francesco Antonio Greco [a], Vincenzo Maione [b], Chiara Custodi [a], Federica Ianni [a], Ursula Grohmann [d], Ciriana Orabona [d], Francesca Cantini [b, c], Antonio Macchiarulo [a, *]

[a] Department of Pharmaceutical Sciences, University of Perugia, Via del Liceo 1, 06123 Perugia, Italy
[b] Center for Magnetic Resonance, University of Florence, Via L. Sacconi 6, 50019 Sesto Fiorentino (FI), Italy
[c] Department of Chemistry, University of Florence, Via della Lastruccia 3, 50019 Sesto Fiorentino (FI), Italy
[d] Department of Experimental Medicine, University of Perugia, P.le Gambuli, 06132 Perugia, Italy

ARTICLE INFO

Article history:
Received 20 July 2017
Received in revised form
20 September 2017
Accepted 21 September 2017
Available online 3 October 2017

Keywords:
Tryptophan
IDO
Inhibitor
Immune
Cancer
Fragment-based
Water-LOGSY
Thermophoresis

ABSTRACT

Indoleamine 2,3-dioxygenase 1 (IDO1) is attracting a great deal of interest as drug target in immune-oncology being highly expressed in cancer cells and participating to the tumor immune-editing process. Although several classes of IDO1 inhibitors have been reported in literature and patent applications, only few compounds have proved optimal pharmacological profile in preclinical studies to be advanced in clinical trials. Accordingly, the quest for novel structural classes of IDO1 inhibitors is still open. In this paper, we report a fragment-based screening campaign that combines Water-LOGSY NMR experiments and microscale thermophoresis approach to identify fragments that may be helpful for the development of novel IDO1 inhibitors as therapeutic agents in immune-oncology disorders.

1. Introduction

Indoleamine 2,3-dioxygenase 1 (IDO1) is a monomeric heme-containing dioxygenase that catalyzes the oxidative cleavage of the essential amino acid L-Tryptophan (L-Trp, **1**, Fig. 1) in the first and rate limiting step of the kynurenine pathway (KP), which accounts for more than 95% of L-Trp catabolism in humans [1]. Two additional enzymes catalyze L-Trp metabolism, namely indoleamine 2,3-dioxygenase 2 (IDO2) and tryptophan 2,3-dioxygenase (TDO), albeit they are endowed with limited structural similarities and diverse biological roles from IDO1 [2]. Among the three enzymes, IDO1 is the most functionally characterized isoform in the regulation of immune responses since the pioneering work of Hayaishi and coworkers, which uncovered the induction of the enzyme as part of the immune control to pathogen infections leading to thwart pathogen growth [3]. In 1998, the breakthrough discovery about the relevance of IDO1 in protecting the fetus from maternal immunity led to depict a major role of the enzyme in the regulation of immunosuppressive pathways [4]. This finding prompted the association of elevated expression of IDO1 in various human cancers to the participation of the enzyme in the tumor immuno-editing process, which sets up peripheral tolerance to tumor antigens [5]. The main mechanisms ascribed to the immunoregulatory functions of IDO1 are the depletion of L-Trp levels and the production of bioactive kynurenine metabolites [6].

Over the last decade, IDO1 has attracted a great deal of interest from pharmaceutical companies and academic research groups aimed at developing novel drugs by controlling immunosuppressive pathways [7]. Intense endeavors have thus been devoted by medicinal chemists to design and develop enzymatic inhibitors, yielding different chemical classes of ligands that are reported in patent applications and/or scientific literature [8].

Notwithstanding the large variety of IDO1 inhibitors hitherto generated, only few of them have made their progress in clinical settings (**2**–**6**, Fig. 1), with epacadostat (**3**) being the advanced candidate in phase III clinical trials as combination therapy with the

* Corresponding author.
E-mail address: antonio.macchiarulo@unipg.it (A. Macchiarulo).
[1] These authors equally contributed to the work.

https://doi.org/10.1016/j.ejmech.2017.09.044

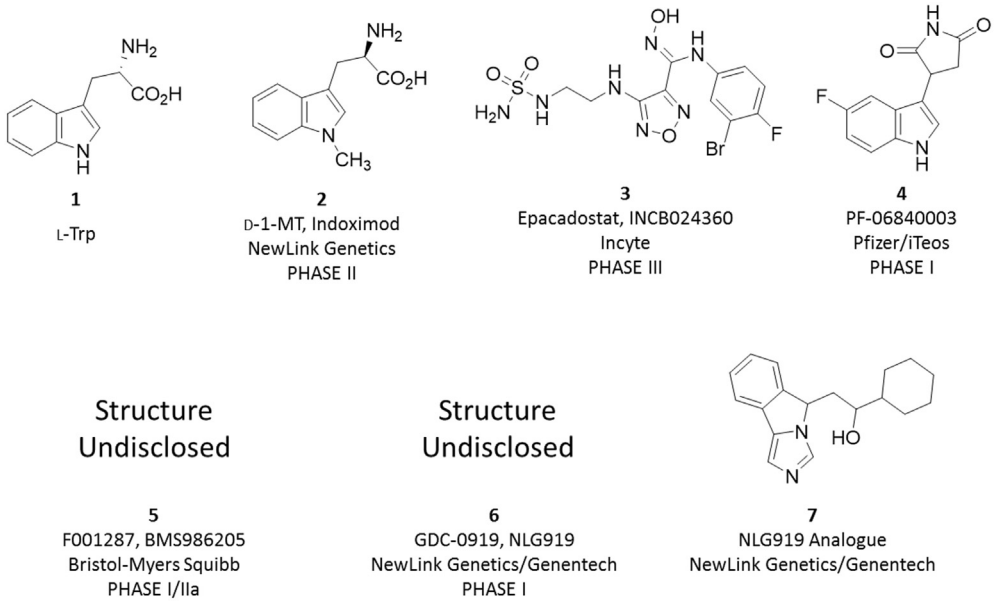

Fig. 1. Chemical structures of L-Trp (**1**) and IDO1 inhibitors (**2**–**7**).

check-point inhibitor pembrolizumab for metastatic melanoma (ClinicalTrials.gov: NCT02752074) [9]. This prompts the quest for novel IDO1 inhibitors that may prove optimal pharmacokinetic and pharmacological profiles for clinical development.

Fragment-based approach relies on the paradigm of screening small collections of chemical compounds, having usually less than 20 heavy atoms, and is a more effective strategy to successfully sample the huge diversity of the chemical space for novel active chemical scaffolds against a given target [10]. This approach is based on the implementation of biophysical techniques as key assays in the screening campaign [11].

In the current paper, we report the results of a screening campaign that combines Water-LOGSY NMR experiments and microscale thermophoresis assay to identify fragments that may be used as starting points for optimization of novel inhibitors against IDO1. In the first step, a collection of commercially available fragments was docked into the crystal structure of IDO1. Next, Water-LOGSY NMR experiments and microscale thermophoresis analysis (MST) were applied to confirm the enzyme binding properties of selected virtual hits. Finally, characterization of key physicochemical properties and early appraisal of functional activity in cellular assays were carried out to prioritize best fragments to be progressed for the development of novel lead compounds for IDO1 inhibition.

2. Methods

2.1. Docking studies

The crystal structure of IDO1 (PDB codes: 2D0T, resolution = 2.30 Å) [12] was downloaded from the Protein Data Bank [13], and its chain A was prepared by adding hydrogen atoms with relative ionization states at pH 7.0, using the Protein Preparation Wizard implemented in of Maestro v10.1 [14]. The unsolved loop 361–379 was reconstructed with Prime v3.9 [15], while the formal charge of the iron was set as Fe^{III}. A virtual library of 30,701 commercially available fragments was assembled selecting compounds compliant to fragment-like criteria (MW $\leq$ 300 and $_{calc}$LogP $\leq$ 3.0) [16] and removing pan-assay interference compounds (PAINS filters) [17] from the corporate collection of Life Chemicals (v2013, about 366,000 compounds). Specifically, MW and $_{calc}$LogP descriptors were calculated using the calculator plugin Marvin v6.2.2, whereas PAINS descriptors were calculated using Canvas v1.7.014 [18]. This library was then processed for docking studies with LigPrep v3.3, generating all ionization and tautomer states at pH 7 ± 2. Docking studies were carried out using Glide v6.6 with the default standard precision (SP) setting combined with expanded sampling mode [18]. A good performance of this docking protocol has been reported in literature for virtual fragment docking [19]. The docking grid was defined with the centre located on the centre of mass of the co-crystallized ligand in 2D0T, and the inner grid box being sized 12 × 12 × 12 Å. Docking solutions with a binding score (Gscore) lower than −7.5 kcal/mol were stored and submitted to clustering analysis. This was carried out in Canvas v1.7 using fingerprint descriptors (Molprint2D) and K-means algorithm, setting a number of 100 expected clusters, 10 runs composed of 20 steps each run, and a cost convergence of 0.0001. A total of 82 clusters were obtained as a result of clustering analysis.

2.2. NMR water-ligand observed via gradient NMR spectroscopy (Water-LOGSY)

This method is based on a transient NOE experiment and implies transfer of magnetization via an intermolecular NOE and spin diffusion. Specifically, bulk water magnetization is excited and transferred during the NOESY mixing time to the bound ligand via two major mechanisms. The first mechanism relies on direct transfer from bulk water molecules at protein-ligand interface. The second mechanism is a chemical exchange between excited water molecules and protein labile protons (e.g., amide, hydroxyl) which propagates to the bound ligand [20]. The Water-LOGSY spectrum contains the bound-state perturbed magnetization as long as the relaxation time T1 of the ligand is greater than the dissociation rate constant k_{off}. In this context, opposite signs for signals from unbound versus protein-bound ligands are observed in a Water-LOGSY spectrum, which enables to easily discriminate between binders and non-binders.

The recombinant protein construct of human IDO1 (rhIDO1,

residues 1–403) was purchased from Giotto Biotech (Giotto Biotech S.r.l., Firenze). Unlabeled IDO1 samples were prepared in phosphate buffer (20 mM, pH 7.2) and no reducing agent such as dithionite was added to the samples. In all experiments, the iron metal ion was therefore in the oxidized form Fe^{III}. Samples for Water-LOGSY experiments were 10 μM in protein concentration and 800 μM in candidate compound concentration.

Water-LOGSY experiments were recorded at 298 K on a Bruker AVANCE 700 MHz spectrometer equipped with a 5 mm triple-resonance TXI, Z-gradient probe, and an automatic sample changer. For each compound, a reference 1D 1H Water-LOGSY spectrum of the compound alone and a 1D 1H Water-LOGSY spectrum of it in the presence of protein was recorded. The initial setup of the Water-LOGSY experiment was performed on the NLG-919 analogue (**7**). Specifically, compound 7 was selected as reference compound given the following observations: (i) it is a potent IDO1 inhibitor (IC_{50} = 38 nM) [21]; (ii) the binding mode of **7** to IDO1 is experimentally available and shows a direct coordinative interaction to the sixth coordination site of ferric heme [21]; (iii) it has been used as reference compound in other studies to validate high-throughput screening assay for IDO1 inhibition and develop immunostimulatory nanomicellar carrier [22,23]; (iv) the chemical structure of **7** could be identical to GDC0919 (**6**), as reported in some catalogues of commercially available inhibitors [24]. The Water-LOGSY experiment of the NLG-919 analogue (**7**) provided an internal control of the reliability of our methodological approach. Experiments were performed with an 180° inversion pulse applied over the water signal at ~4.7 ppm by means of a Gaussian-shaped selective pulse of 10 ms. Each Water-LOGSY spectrum was acquired with 1 K scans.

Water-LOGSY NMR spectra of selected compounds **8**, **15** and **18**, are reported in supplementary materials (Figs. S1–S3).

2.3. Microscale thermophoresis (MST)

Thermophoresis is the movement of a biomolecular complex in a temperature gradient depending on size, charge, and hydration shell that typically change upon ligand/target interaction [25]. The MST experiment is based on the use of 16 capillary tubes that are filled with a fluorescent dye-labeled target protein and a serial titration of unlabeled ligand. Capillary tubes are then illuminated with an infrared laser that generates a temperature gradient. The protein/ligand complex migrates along this gradient causing changes in the observed fluorescence. These are used to generate a binding curve as a function of ligand concentration that is then analyzed to assess the K_d value.

Fluorescence labeling of rhIDO1 was performed following the protocol for N-hydroxysuccinimide (NHS) coupling of the dye NT647 (NanoTemper Techonologies, Munich) to lysine residues. Briefly, 100 μL of a 9.95 μM solution of rhIDO1 protein in labeling buffer (130 mM $NaHCO_3$, 50 mM NaCl, pH 8.2) was mixed with 100 μL of 39.8 μM NT647-NHS fluorophore (NanoTemper Technologies) in labeling buffer and incubated for 30 min at room temperature (RT) in the dark. Unbounded fluorophores were removed by size-exclusion chromatography with MST buffer (50 mM TRIS, 150 mM NaCl, 10 mM $MgCl_2$, pH 7.4, 0.05% Tween20) as running buffer. The real concentration of each element of the sample, such as protein, heme group and RED dye, and the degree of labeling (DOL) were determined using extinction coefficient ε280 = 51,380 M^{-1} cm^{-1} for rhIDO1, ε405 = 159,000 M^{-1} cm^{-1} for rhIDO1 heme group and ε650 = 250,000 M^{-1} cm^{-1} for NT647 fluorophore, with a correction factor of Fcorr of 0.028 at 280 nm, using Cprot = [A280 − (A280 x Fcorr)/ε280 x l] and DOL resulted between 0.6 and 0.8 throughout all labeling reactions.

The stability of NT647-rhIDO1 and unmodified rhIDO1 protein was checked using circular dicroism. Spectra of both proteins were recorded using Jasco810 spectrophotometer with 1 mm path-length quartz cuvettes at room temperature (≈22 °C). Sensitivity was 100 millidegrees, and the scanning speed was 20 nm/min for an accumulation of 2 scans. CD data were collected between 180 and 260 nm for both samples at a concentration of 0.1 mg/ml in phosphate buffer (PPB; 50 mM K_2HPO_4, pH 7.4) Deconvolution of spectra was performed with CDNN 2.1 software. Results are reported in the supplementary materials (Table S1).

Compound screening was carried out using premium-coated capillary and MST buffer including 2% DMSO and 2 mM DTT. Compound stocks (50 mM) in DMSO were diluted in assay buffer to reach a final maximum concentration of 500 μM or 1 mM, depending on compound solubility. Compound pre-dilutions were prepared for MST experiments by 16-fold 1:1 serial dilutions in assay buffer containing 4% DMSO in PCR tubes (supplied by NanoTemper Technologies) to yield final volumes of 10 μL. A solution of NT647-rhIDO1 at a concentration of 90 nM was prepared and 10 μL of this solution was added to each compound dilution to reach a final NT647-rhIDO1 concentration of 45 nM and a reaction volume of 20 μL. These samples were loaded into 16 premium-coated capillary tubes and inserted in the chip tray of the MST instrument (Monolith NT.115) for thermophoresis analysis and the appraisal of K_d values. MST signals were recorded at MST 40% (compounds **7**, **9**, **10**, **23**, **28**). Compounds not providing a binding curve with a good signal/noise ratio at 40% (**8**, **11**–**22**, **24**–**27**, **29**) were tested at MST 80%. In both cases, a 20% LED power was used. K_d values were calculated from compound concentration-dependent changes in normalized fluorescence (Fnorm) of NT647-rhIDO1 after 21s of thermophoresis at MST 40% and after 4s at MST 80%. Each compound was tested in triplicate samples and data analyzed using *MO Affinity Analysis* software (NanoTemper Technologies). Confidence values (±) are indicated next to K_d value for each of tested compound. Specifically, confidence values define the range where the K_d falls with a 68% of certainty. The binding efficiency index (BEI) of each fragment was calculated with the following equations: (eq. 1) BEI = pK_d/MW [26].

2.4. Cellular assay

P1.HTR, a highly transfectable clonal variant of mouse mastocytoma P815 [27] was cultured in Iscove's Modified Dulbecco's Medium supplemented with 10% FCS. P1.HTR cells were transfected by electroporation with plasmid constructs coding for murine IDO1 (P1.IDO1). A stable transfectant cell line was obtained by puromycin selection. Cells at the concentration of 0.1 × 10^6 cell/ml were incubated with 30 μM of compounds for 16 h. Control was represented by cells incubated with an equivalent volume of DMSO (the vehicle in which compounds were solubilized). After the incubation, supernatants of cell cultures were recovered and kynurenine concentration was detected by HPLC. Dose-response curves were built through the same cellular assay, incubating P1.IDO1 cells with serial dilutions of molecules, starting from 30 μM. All the experiments were conducted in triplicate and repeated almost two times. Results are represented as the mean ± standard deviation of the kynurenine fold change (L-Kyn FC), meaning the ratio between kynurenine concentration secreted in the supernatant of the compound-treated versus vehicle-treated cells.

2.5. Physicochemical properties

Calculator plugins were used for $_{calc}$pKa and $_{calc}$logP property prediction [28]. Experimental pKa ($_{exp}$pKa) and logP ($_{exp}$logP) were determined for compounds **7**, **8**, **15**, and **18**. Specifically, each experiment was performed with Sirius T3, specifying sample

weight, number of expected pKa values, predicted pKa values, number of three titrations, and titration mode. In order to measure the pKa of a compound, a sample concentration of 1 mM was prepared. Poor soluble compounds were dissolved adding methanol as co-solvent. In this case, three titrations were performed at different methanol/water ratios (50% methanol, 40% methanol, and 30% methanol) in order to determine aqueous pKa. The Yasuda-Shedlovsky method was chosen to extrapolate aqueous pKa values. The R^2 value was used to evaluate the validity of the assay with co-solvent, and results were considered acceptable with R^2 value $\geq$ 0.9. Conversely, root mean square deviation (rmsd) value was used to assess the quality of experiments performed for high soluble compounds dissolved without co-solvent. Results were analyzed using Sirius T3 software v1.1.0.5. Experimental logP values were determined using pH-metric assays in *n*1-octanol and water. Since $_{calc}$logP values were comprised between 1 and 3, a pH-metric medium logP model was used as determination method.

2.6. Compound purity and integrity

All tested compounds were purchased from Life Chemicals. Active fragments **8**, **15** and **18** were further tested for purity ($\geq$95%) and structural integrity using HPLC and 1H NMR (see supplementary materials, Figs. S4–S9).

3. Results

3.1. Docking studies

A library of commercially available fragments was assembled selecting compounds compliant to fragment-like criteria (MW $\leq$ 300 and cLogP $\leq$ 3.0) [16] from the corporate collection of Life Chemicals, and removing pan-assay interference compounds (PAINS filters) [17] After this procedure, 30,701 fragments were obtained and used for docking studies.

Because the virtual library contained fragment-like molecules, we used a docking procedure specifically validated for generating protein-fragment complexes [19] Accordingly, each of the 30,701 compounds was docked into the catalytic pocket of IDO1 (PDB ID: 2D0T) using Glide with expanded sampling mode. About 800,000 solutions were generated including compounds with multiple binding poses to the enzyme. These were filtered by means of selecting solutions with a binding score (Gscore) lower than −7.5 kcal/mol that were eventually clustered using fingerprint descriptors as reported in the method section.

Within each of the resulting 82 clusters (Fig. 2), a representative compound endowed with the best Gscore was selected and further cherry-picked according to the criteria of readily availability for purchasing. As a consequence, a total of 59 virtual hits were acquired and used for NMR Water-LOGSY screening.

3.2. Water-LOGSY NMR experiments

Water-LOGSY NMR screening was carried out as detailed in the method section for assessing the binding of 59 compounds to IDO1. The peak intensity variation was calculated between 1D Water-LOGSY spectrum of the small molecule alone, taken as reference value, and 1D Water-LOGSY spectrum in the presence of the enzyme. Specifically, peak intensity variation less than 90% between the two spectra was considered not significant and typical for weak or non-interacting molecules; a decrease of the signal intensity in the 90–100% range and NMR signals with opposite sign in 1D Water-LOGSY spectrum were taken as indication of ligand binders.

As a result, 22 small molecules showed significant peak intensity variation (**8**–**29,** Figs. 3 and 4), with 15 of them being endowed with a strong-binding signature (opposite sign, Table 1). These compounds were used in MST binding assay with the aim of determining their equilibrium dissociation constants (K_d) to IDO1.

3.3. Microscale thermophoresis experiments

Using MST, we analyzed the binding of each of the 22 fragments (**8**–**29**) to IDO1. Before running the experiments, IDO1 was labeled with a fluorescent dye (NT647-IDO1) and its stability was checked using circular dichroism to verify that the fluorescent label had not compromised protein stability (supplementary materials, Table S1). Buffer conditions were evaluated to identify optimal state for MST signal reproducibility and the suppression of unspecific adsorption to capillary walls. NT647-IDO1 functionality was assessed by quantifying its interaction with NLG919 analogue (**3**), yielding K_d values of 3.30 ± 0.40 μM. MST screening of the 22 compounds was performed as detailed in the method section, and results are reported in Table 1. The analysis revealed that eight compounds do not show any binding activity at the maximum tested concentration of 1 mM. One compound (**15**) showed binding activity with K_d below 30 μM, whereas remaining compounds displayed weaker K_d values, i.e. ranging from 30 μM to 900 μM. Ligand binding efficiency is an index based on molecular weight (MW) that provides an effective ranking of fragments to aid prioritization on the route to generate lead compounds [20]. The binding efficiency index (BEI) was calculated for each of the tested fragments. Of note, compounds **15** and **20** were found to be endowed with a BEI higher than that of the reference IDO1 inhibitor **7**, while compounds **14** and **16** showed similar BEI to the known inhibitor.

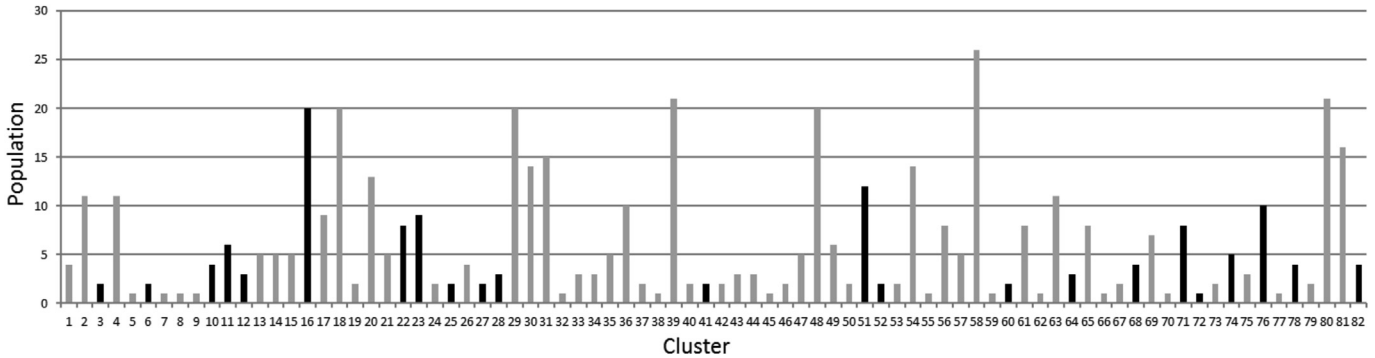

Fig. 2. Clusters of binding poses obtained from docking studies of the collected fragment library into the catalytic pocket of IDO1. Gray and black bars indicate clusters containing at least one compound available or not available for purchasing, respectively.

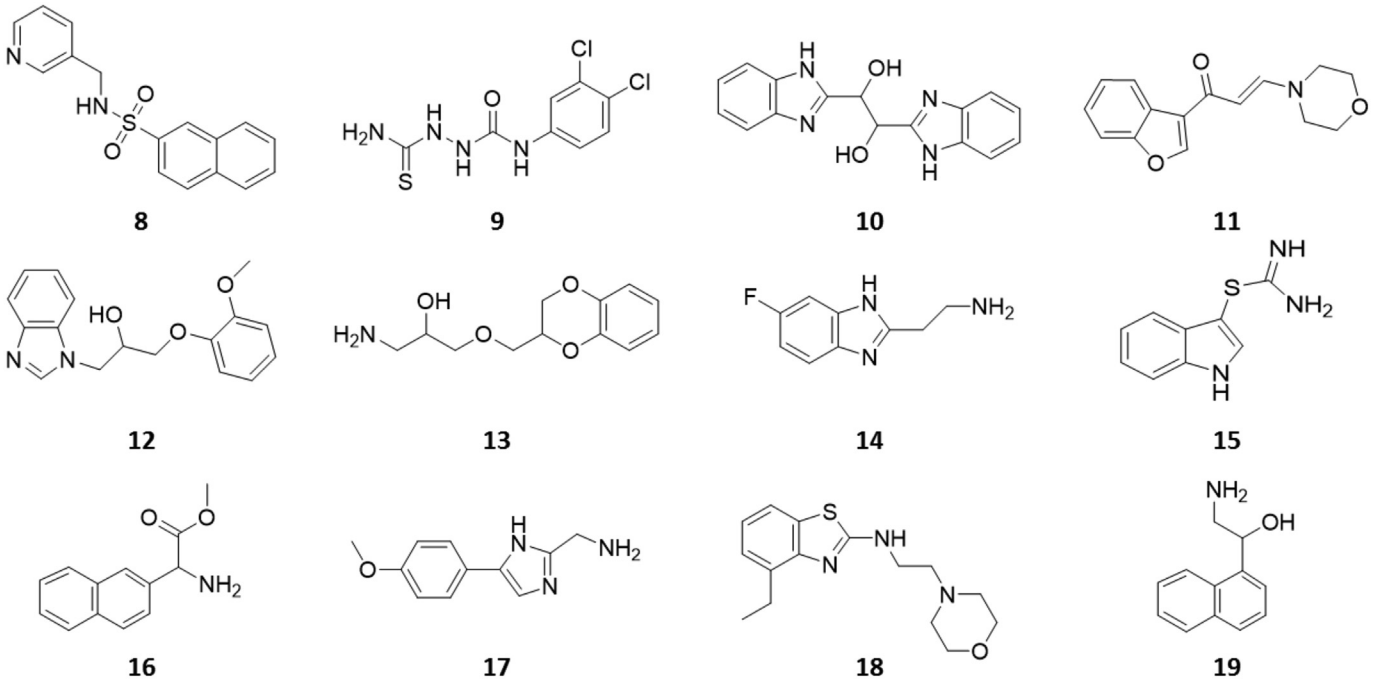

Fig. 3. Chemical structures of fragments **8**–**19**.

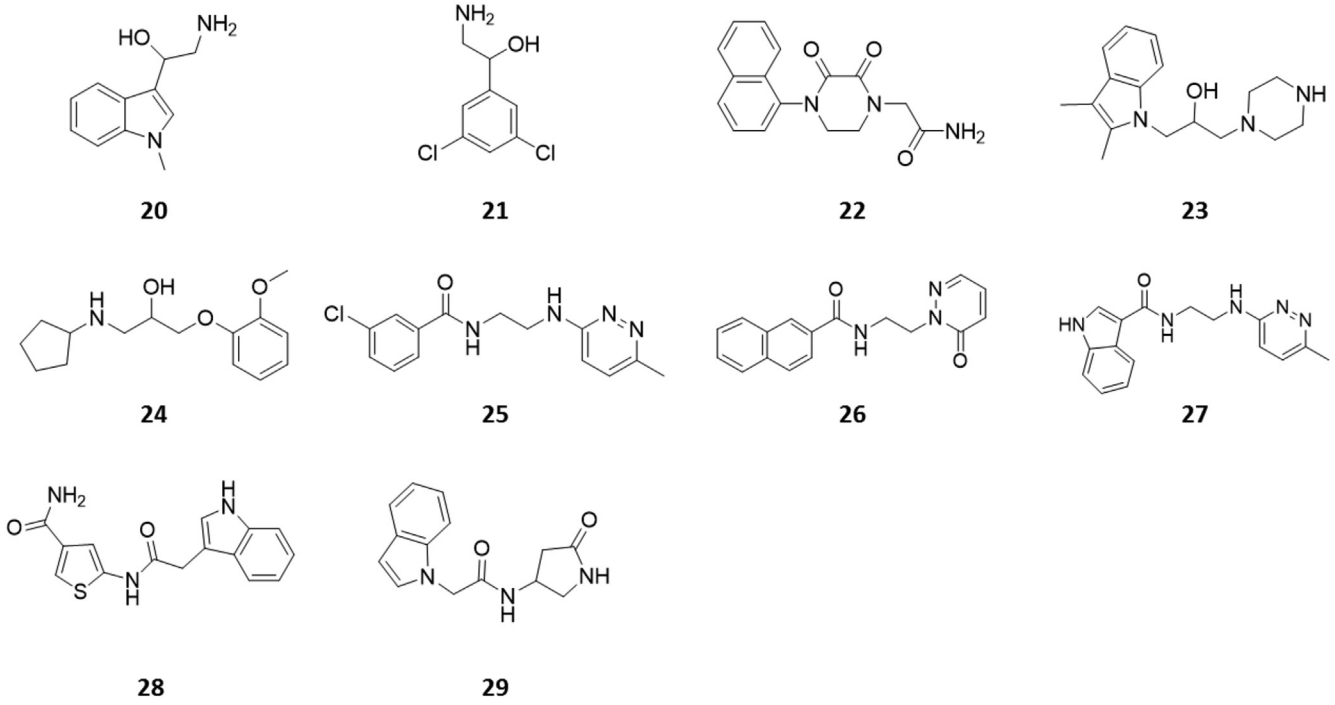

Fig. 4. Chemical structures of fragments **20**–**29**.

3.4. Physicochemical properties

Calculated and experimental acidic constant ($_{calc}$pKa, $_{exp}$pKa) and *n*-octantol/water partition coefficient ($_{calc}$logP, $_{exp}$logP) were assessed for the NLG919 analogue (**3**) and selected fragments with the lowest K_d values **8**, **15**, and **18** (Table 2), before progressing them to cellular assay. Specifically, $_{calc}$logP and $_{exp}$logP values were used to estimate the lipophilicity of the compounds and infer their passive absorption capability in cells. Values of $_{exp}$pKa and $_{exp}$logP were determined through a Sirius T3 instrument as reported in the method section. All tested compounds show a $_{exp}$logP in the range between 1.8 and 3.2, wherein it is expected a good balance between passive permeability and solubility. Moreover, a fair correlation between experimental and calculated values was also obtained, with only compound **18** displaying a lower $_{exp}$logP with respect to $_{calc}$logP.

Table 1
Molecular weights (MW), NMR peak variations and affinity constants (K_d) of reference compound **7** and fragments **8**–**29**.

Compound	Code	MW	NMR Peak Variation	MST K_d (μM)	BEI
7	NLG919 analogue	282	opposite sign	3.3 ± 0.4	19
8	VIS201	298	opposite sign	53.7 ± 14.2	14
9	VIS202	279	opposite sign	941 ± 185	11
10	VIS205	294	opposite sign	774 ± 104	11
11	VIS208	257	opposite sign	147 ± 61	15
12	VIS207	298	opposite sign	86.8 ± 31.1	14
13	VIS209	239	100%	>1000	–
14	VIS212	179	opposite sign	548 ± 127	18
15	VIS210	191	opposite sign	17.8 ± 3.9	25
16	VIS217	215	opposite sign	169 ± 76	18
17	VIS219	203	opposite sign	>500	–
18	VIS220	291	100%	33.5 ± 7.7	15
19	VIS221	187	100%	>1000	–
20	VIS225	190	opposite sign	97.0 ± 51.0	21
21	VIS228	206	opposite sign	>1000	–
22	VIS234	295	100%	>1000	–
23	VIS237	287	opposite sign	96.7 ± 51.1	14
24	VIS238	265	opposite sign	>1000	–
25	VIS245	290	opposite sign	>1000	–
26	VIS243	293	100%	240 ± 58	12
27	VIS246	295	opposite sign	>1000	–
28	VIS248	299	90%	61.5 ± 10.6	14
29	VIS253	257	100%	237 ± 116	14

Table 2
Experimental and calculated physicochemical properties of reference compound **7** and active fragments **8, 15** and **18**.

Compound	VIS	$_{exp}$logP	$_{calc}$logP	$_{exp}$pKa	$_{calc}$pKa
7	NLG919 analogue	3.2	3.0	6.7	6.3
8	VIS201	2.5	2.3	4.8/10.3	4.8/10.1
15	VIS210	1.8	1.9	9.5	9.6
18	VIS220	2.3	3.0	3.1/6.2	3.0/6.4

3.5. Cellular assay experiments

NLG919 analogue (**7**) and the selected fragments **8**, **15,** and **18** (Fig. 5) were tested in cellular assay for their ability to cross cell membrane and inhibit IDO1 catalytic activity. The cell line of murine mastocytoma P1.HTR stably transfected with murine IDO1 (P1.IDO1) was cultured for 16 h in the presence of each compound at the concentration of 30 μM. The ability of P1.IDO1 cells to convert L-Trp — contained in the culture medium at the concentration of 78.4 μM — into L-Kyn was then assessed after 16 h of incubation. Results are reported in Fig. 6A as fold change of L-Kyn concentration (L-Kyn FC), detected in the supernatants from molecule-incubated as compared to vehicle-incubated cells. As expected, a strong reduction (FC < 0.3) of L-Kyn production was observed in P1.IDO1 after incubation with the reference compound **7**, being this molecule a potent IDO1 inhibitor. Among selected fragments, only compound **15** significantly reduced L-Kyn production in P1.IDO1 cells with a FC ≤ 0.6. Given the high BEI index of **15** and its functional activity in cellular assays, the IC_{50} value of this fragment was next evaluated along with **7** in P1.IDO1 cells, yielding a value of 14.40 ± 3.70 μM that is lower than 0.013 ± 0.03 μM of the NLG919 analogue (**7**) (Fig. 6b).

4. Discussion

In the last decade, IDO1 has become a relevant checkpoint target in cancer immunotherapy. As a consequence, small molecules inhibiting its catalytic activity are being developed with the aim of potentiating anti-tumor immunity.

In this work, a library of 30,701 fragments was docked into the crystal structure of IDO1 as reported in the method section. Fragments featuring a docking score (Gscore) better than −7.5 kcal/mol were selected and clustered using fingerprint descriptors. As a result, 82 groups of fragments were found, and one representative compound with the best Gscore was preselected for each cluster and further cherry-picked according to criteria of readily availability for purchasing. A total of 59 virtual hits was thus acquired and used for NMR Water-LOGSY screening, which confirmed the interaction with IDO1 for 22 fragments (hit rate 37%). Structurally, active compounds comprised heterogeneous chemical classes, including ethanolamine (**13**, **19**, **20**, **21**, **23**, **24**), sulfonamide (**8**), amide (**22**, **25**–**29**), aminoacid (**16**), benzoimidazole (**10**, **12**, **14**), benzofurane (**11**), benzothiazole (**18**), indole (**15**, **20**, **23**, **28**, **29**), and imidazole (**17**) derivatives, with some indole fragments (**23**, **28**, **29**) belonging to multiple classes. These fragments were next analyzed by MST and 14 hits were found to interact with IDO1 with different dissociation constants, as indicated by compound concentration-dependent changes in thermophoretic movement of NT647-IDO1. In terms of ligand BEI, two indole fragments (**15, 20**) showed efficiencies higher than compound **7**, and two other fragments (**14**, **16**) displayed a BEI index similar to the reference IDO1 inhibitor. It is worth noting that fragment **20** is a structural analogue of D-1-metyhl-tryptophan (D-1MT, **2**), with the β-hydroxyl group of the former replacing the α-carboxylic moiety of the latter.

Although fragments are not required to show activity in functional assays, being starting points for further lead design and optimization efforts, the most active compounds **8, 15** and **18** and reference inhibitor **7** (Fig. 5) were first evaluated for their physicochemical properties, and then tested in cellular assays (Fig. 6). In particular, calculated and experimental physicochemical properties of these compounds (Table 2) suggested a good balance between passive permeability and solubility, supporting their evaluation in cellular assays. This latter experimental appraisal was carried out in the P1.IDO1 cell line that stably expresses the IDO1 enzyme. As a result, only fragment **15** resulted in a reduced L-Kyn secretion by P1-IDO1 with an IC_{50} of 14.40 ± 3.70 μM, and thereby keeping a BEI of 25 in the cellular assay as well. Conversely, the binding activity (K_d) of compounds **8** and **18** was not sufficient to yield functional activity at the tested concentration of 30 μM in the cellular assay. The inspection of the top scored binding pose of fragment **15** from docking studies into the crystal structure of IDO1 revealed minimal interaction features that account for the high binding efficiency of this compound against the enzyme both *in vitro* and cellular conditions (Fig. 7A). Specifically, the indole moiety is placed over the heme group, with the nitrogen atom engaging Ser167 in one hydrogen bond and the aromatic ring making π-π contacts with Phe163 and Tyr126. The isothiourea side chain forms two electrostatic enforced hydrogen bonds with one propionate group of the heme cofactor. In the case of fragment **8**, the top scored binding pose showed the sulfonamide moiety making a hydrogen bond with the propionate group of the heme cofactor, while the pyridine group engaged Gly236 and Gly261 in hydrogen bond interactions, and the naphtyl group was placed over the heme plane where it interacts with Phe163 through π-π interactions (Fig. 7B).

Finally, according to the top scored binding pose of fragment **18**, the benzothiazole group was placed over the heme plane establishing π-π interactions with Phe163 and Tyr126, and projecting the ethyl group in C2 position towards the upper part of the catalytic cavity. The morpholin-ethylamine side chain pointed to the entry channel of IDO1 catalytic pocket (Fig. 7C).

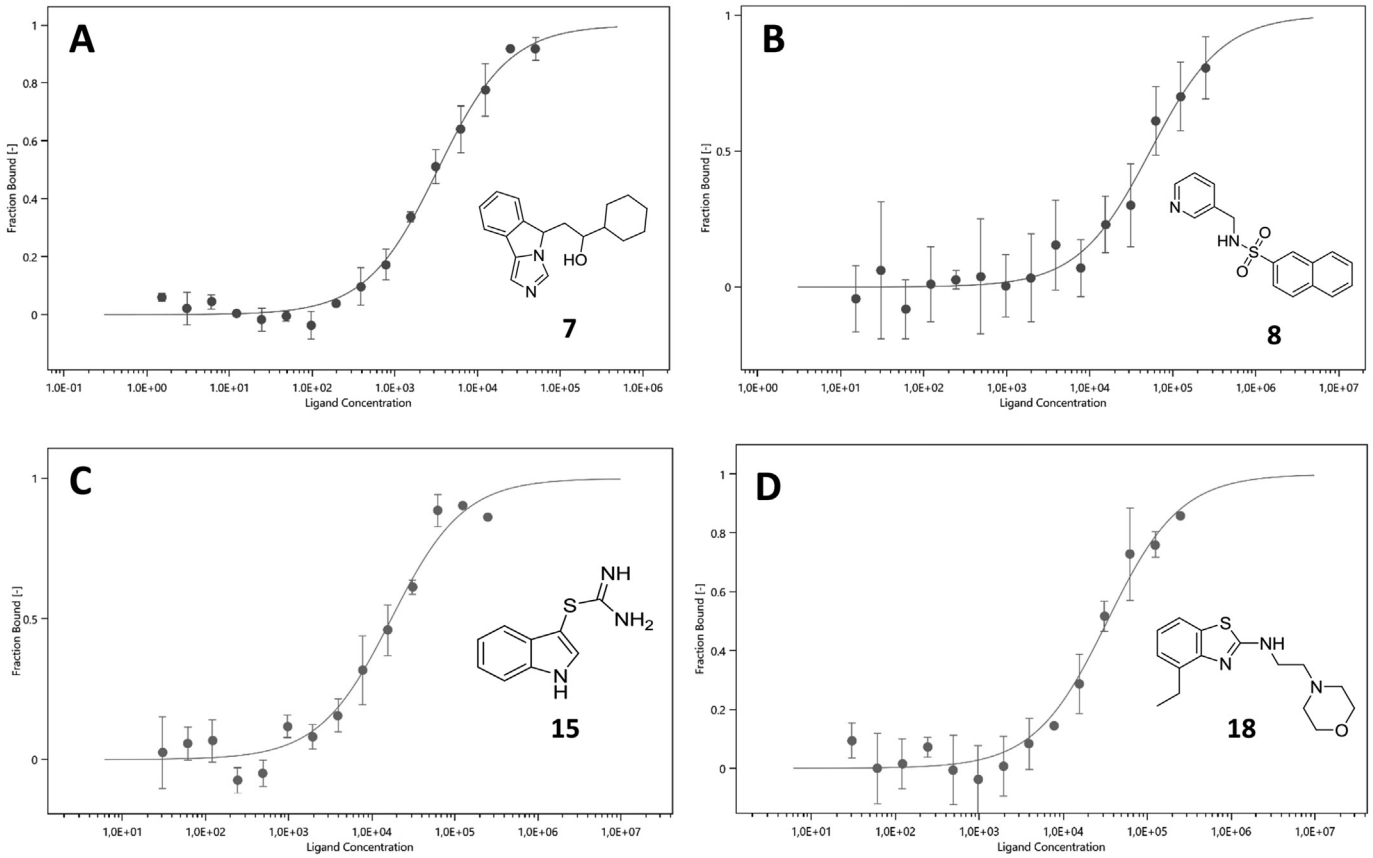

Fig. 5. MST binding curve of protein fraction bound *vs* ligand concentration (nM) for **7** (A), **8** (B), **15** (C) and **18** (D).

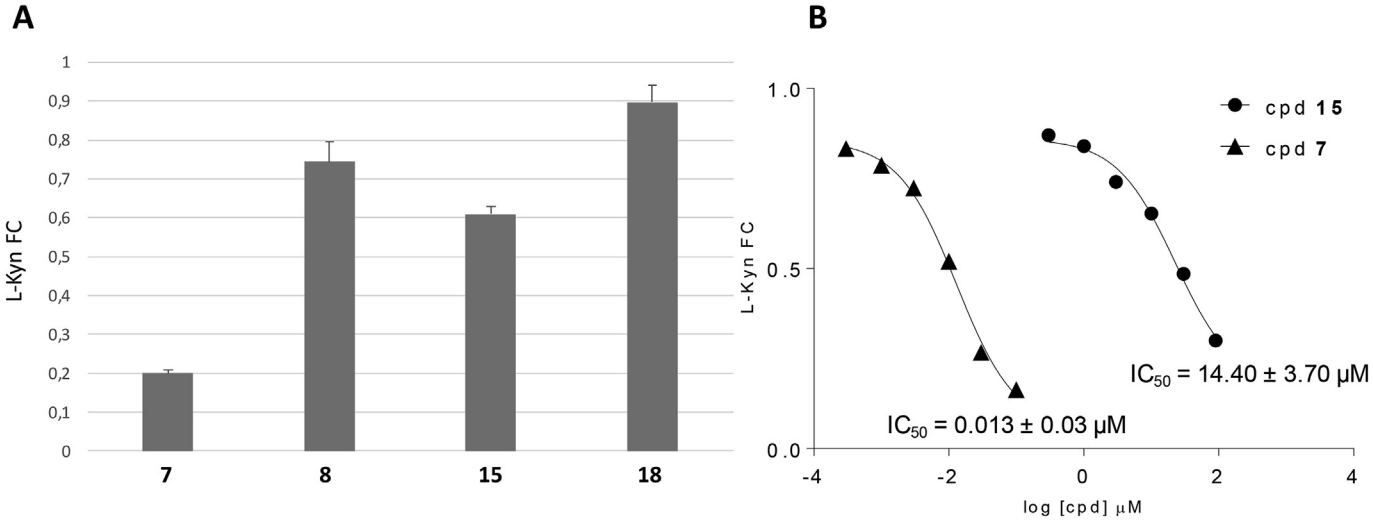

Fig. 6. A) Fold change of L-Kyn concentration (L-Kyn FC) in the supernatants from molecule-incubated compared to vehicle-incubated P1.IDO1 cells. B) Dose-inhibition curve of fragment **15** in P1.IDO1 cells.

5. Conclusion

Targeting IDO1 with small molecule inhibitors offers new therapeutic opportunities for potentiating the immune response against cancer. Despite several classes of inhibitors have been disclosed in literature and patent applications, few compounds have proved an optimal pharmacological profile in preclinical studies to be advanced in clinical trials. In this work, we reported a screening campaign that was based on the use of Water-LOGSY and MST methods to determine the dissociation constant of ligands to IDO1, and next on the appraisal of functional activity of true binders in cellular assays expressing IDO1. The screening campaign enabled the identification of two fragments (**15** and **20**) with BEI higher than the NLG919 analogue (**7**), and three fragments (**8**, **15**, **18**) with

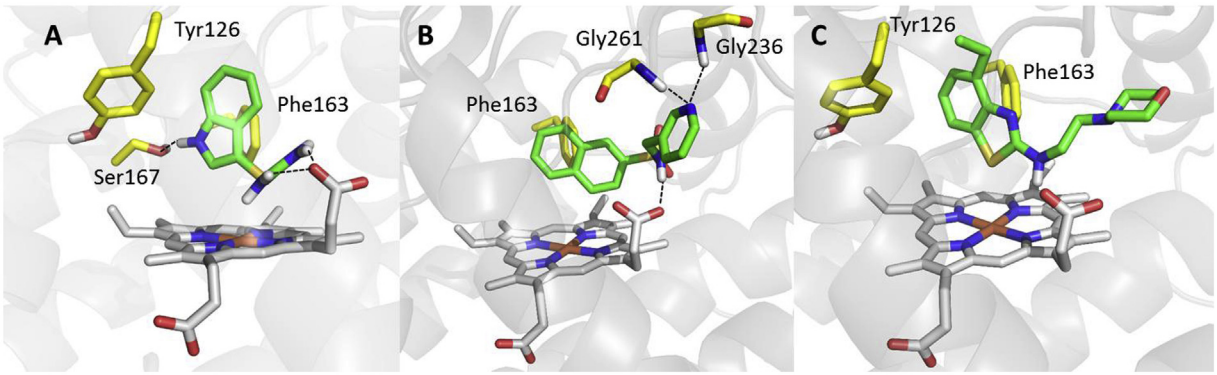

Fig. 7. Top scored binding poses of fragments **15** (A), **8** (B) and **18** (C) into the catalytic pocket of IDO1.

K_d values ranging from 17.8 ± 3.9 μM to 53.7 ± 14.2 μM. These latter compounds were further investigated for their physicochemical properties and IDO1 inhibition activity in P1.IDO1 cells. Results pinpointed the molecule **15** as an interesting fragment for further chemical manipulations towards the design of potent IDO1 inhibitors, being endowed with a high and conserved BEI of 25 both *in vitro* and cellular assays. Notwithstanding, in view of their low molecular weight and binding activity, also fragments **8**, **18** and **20** may still be considered interesting building blocks on the way to develop potent lead compounds for IDO1 modulation.

Acknowledgments

This work was supported by the Italian Ministry of University and Research (PRIN 2012S47X27) to CO, FC and AM, and the European Research Council (ERC-2013-AdG 338954-DIDO) to UG and AM.

Appendix A. Supplementary data

Supplementary data related to this article can be found at https://doi.org/10.1016/j.ejmech.2017.09.044.

References

[1] (a) A.W. Yeung, A.C. Terentis, N.J. King, S.R. Thomas, Role of indoleamine 2,3-dioxygenase in health and disease, Clin. Sci. (Lond) 129 (2015) 601–672;
(b) A.B. Dounay, J.B. Tuttle, P.R. Verhoest, Challenges and opportunities in the discovery of new therapeutics targeting the kynurenine pathway, J. Med. Chem. 58 (2015) 8762–8782;
(c) A. Macchiarulo, E. Camaioni, R. Nuti, R. Pellicciari, Highlights at the gate of tryptophan catabolism: a review on the mechanisms of activation and regulation of indoleamine 2,3-dioxygenase (IDO), a novel target in cancer disease, Amino Acids 37 (2009) 219–229;
(d) G. Mondanelli, S. Ugel, U. Grohmann, V. Bronte, The immune regulation in cancer by the amino acid metabolizing enzymes ARG and IDO, Curr. Opin. Pharmacol. 35 (2017) 30–39.

[2] (a) C.J. Austin, L.M. Rendina, Targeting key dioxygenases in tryptophan-kynurenine metabolism for immunomodulation and cancer chemotherapy, Drug Discov. Today 20 (2015) 609–617;
(b) H.J. Ball, H.J. Yuasa, C.J. Austin, S. Weiser, N.H. Hunt, Indoleamine 2,3-dioxygenase-2; a new enzyme in the kynurenine pathway, Int. J. Biochem. Cell Biol. 41 (2009) 467–471.

[3] a) R. Yoshida, O. Hayaishi, Induction of pulmonary indoleamine 2,3-dioxygenase by intraperitoneal injection of bacterial lipopolysaccharide, Proc. Natl. Acad. Sci. U. S. A. 75 (1978) 3998–4000;
(b) R. Yoshida, Y. Urade, M. Tokuda, O. Hayaishi, Induction of indoleamine 2,3-dioxygenase in mouse lung during virus infection, Proc. Natl. Acad. Sci. U. S. A. 76 (1979) 4084–4086.

[4] D.H. Munn, M. Zhou, J.T. Attwood, I. Bondarev, S.J. Conway, B. Marshall, C. Brown, A.L. Mellor, Prevention of allogeneic fetal rejection by tryptophan catabolism, Science 281 (1998) 1191–1193.

[5] C. Uyttenhove, L. Pilotte, I. Théate, V. Stroobant, D. Colau, N. Parmentier, T. Boon, B.J. Van den Eynde, Evidence for a tumoral immune resistance mechanism based on tryptophan degradation by indoleamine 2,3-dioxygenase, Nat. Med. 9 (2003) 1269–1274.

[6] (a) E.R. Pfefferkorn, Interferon gamma blocks the growth of Toxoplasma gondii in human fibroblasts by inducing the host cells to degrade tryptophan, Proc. Natl. Acad. Sci. U. S. A. 81 (1984) 908–912;
(b) J.R. Moffett, M.A. Namboodiri, Tryptophan and the immune response, Immunol. Cell Biol. 81 (2003) 247–265;
(c) A.A. Badawy, A.M. Namboodiri, J.R. Moffett, The end of the road for the tryptophan depletion concept in pregnancy and infection, Clin. Sci. (Lond) 130 (2016) 1327–1333.

[7] (a) C. Sheridan, IDO inhibitors move center stage in immuno-oncology, Nat. Biotechnol. 33 (2015) 321–322;
(b) F.A. Greco, A. Coletti, E. Camaioni, A. Carotti, M. Marinozzi, A. Gioiello, A. Macchiarulo, The Janus-faced nature of IDO1 in infectious diseases: challenges and therapeutic opportunities, Future Med. Chem. 8 (2016) 39–54.

[8] (a) E. Dolušić, R. Frédérick, Indoleamine 2,3-dioxygenase inhibitors: a patent review (2008-2012), Expert Opin. Ther. Pat. 23 (2013) 1367–1381;
(b) T. Jiang, Y. Sun, Z. Yin, S. Feng, L. Sun, Z. Li, Research progress of indoleamine 2,3-dioxygenase inhibitors, Future Med. Chem. 7 (2015) 185–201;
(c) A. Coletti, F.A. Greco, D. Dolciami, E. Camaioni, R. Sardella, M.T. Pallotta, C. Volpi, C. Orabona, U. Grohmann, A. Macchiarulo, Advances in indolemine 2,3-dioxygenase 1 medicinal chemistry: structure-function and structure-activity relationships of the enzyme and its inhibitors, MedChemComm 8 (2017) 1378–1392.

[9] (a) H.H. Soliman, E. Jackson, T. Neuger, E.C. Dees, R.D. Harvey, H. Han, R. Ismail-Khan, S. Minton, N.N. Vahanian, C. Link, D.M. Sullivan, S. Antonia, A first in man phase I trial of the oral immunomodulator, indoximod, combined with docetaxel in patients with metastatic solid tumors, Oncotarget 5 (2014) 8136–8146;
(b) E. Vacchelli, F. Aranda, A. Eggermont, C. Sautès-Fridman, E. Tartour, E.P. Kennedy, M. Platten, L. Zitvogel, G. Kroemer, L. Galluzzi, Trial watch: IDO inhibitors in cancer therapy, Oncoimmunology 3 (2014) e957994;
(c) E.W. Yue, R. Sparks, P. Polam, D. Modi, B. Douty, B. Wayland, B. Glass, A. Takvorian, J. Glenn, W. Zhu, M. Bower, X. Liu, L. Leffet, Q. Wang, K.J. Bowman, M.J. Hansbury, M. Wei, Y. Li, R. Wynn, T.C. Burn, H.K. Koblish, J.S. Fridman, T. Emm, P.A. Scherle, B. Metcalf, A.P. Combs, INCB24360 (epacadostat), a highly potent and selective indoleamine-2,3-dioxygenase 1 (IDO1) inhibitor for immuno-oncology, ACS Med. Chem. Lett. 8 (2017) 486–491.

[10] D.A. Erlanson, S.W. Fesik, R.E. Hubbard, W. Jahnke, H. Jhoti, Twenty years on: the impact of fragments on drug discovery, Nat. Rev. Drug Discov. 15 (2016) 605–619.

[11] J.P. Renaud, C.W. Chung, U.H. Danielson, U. Egner, M. Hennig, R.E. Hubbard, H. Nar, Biophysics in drug discovery: impact, challenges and opportunities, Nat. Rev. Drug. Discov. 15 (2016) 679–698.

[12] H. Sugimoto, S. Oda, T. Otsuki, T. Hino, T. Yoshida, Y. Shiro, Crystal structure of human indoleamine 2,3-dioxygenase: catalytic mechanism of O2 incorporation by a heme-containing dioxygenase, Proc. Natl. Acad. Sci. U. S. A. 103 (2006) 2611–2616.

[13] H.M. Berman, J. Westbrook, Z. Feng, G. Gilliland, T.N. Bhat, H. Weissig, I.N. Shindyalov, P.E. Bourne, The protein Data Bank, Nucleic Acids Res. 28 (2000) 235–242.

[14] Maestro, Version 10.1, Schrödinger, LLC, New York, NY, 2015.

[15] Prime, Version 3.9, Schrödinger, LLC, New York, NY, 2015.

[16] M. Congreve, R. Carr, C. Murray, H. Jhoti, A "rule of three" for fragment-based lead discovery? Drug Discov. Today 8 (2003) 876–877.

[17] J.B. Baell, G.A. Holloway, New substructure filters for removal of pan assay interference compounds (PAINS) from screening libraries and for their exclusion in bioassays, J. Med. Chem. 53 (2010) 2719–2740.

[18] (a) Canvas, Version 1.7.014, Schrödinger, LLC, New York, NY, 2015;
(b) Glide, Version 6.6, Schrödinger, LLC, New York, NY, 2015.

[19] M. Sándor, R. Kiss, G.M. Keseru, Virtual fragment docking by Glide: a validation study on 190 protein-fragment complexes, J. Chem. Inf. Model 50 (2010)

1165–1172.
[20] C. Dalvit, P. Pevarello, M. Tatò, M. Veronesi, A. Vulpetti, M. Sundströmet, Identification of compounds with binding affinity to proteins via magnetization transfer from bulk water, J. Biomol. NMR 18 (2000) 65–68.
[21] Y.H. Peng, S.H. Ueng, C.T. Tseng, M.S. Hung, J.S. Song, J.S. Wu, F.Y. Liao, Y.S. Fan, M.H. Wu, W.C. Hsiao, C.C. Hsueh, S.Y. Lin, C.Y. Cheng, C.H. Tu, L.C. Lee, M.F. Cheng, K.S. Shia, C. Shih, S.Y. Wu, Important hydrogen bond networks in indoleamine 2,3-dioxygenase 1 (IDO1) inhibitor design revealed by crystal structures of imidazoleisoindole derivatives with IDO1, J. Med. Chem. 59 (2016) 282–293.
[22] N. Seegers, A.M. van Doornmalen, J.C. Uitdehaag, J. de Man, R.C. Buijsman, G.J. Zaman, High-throughput fluorescence-based screening assays for tryptophan-catabolizing enzymes, J. Biomol. Screen 19 (2014) 1266–12674.
[23] Y. Chen, R. Xia, Y. Huang, W. Zhao, J. Li, X. Zhang, P. Wang, R. Venkataramanan, J. Fan, W. Xie, X. Ma, B. Lu, S. Li, An immunostimulatory dual-functional nanocarrier that improves cancer immunochemotherapy, Nat. Commun. 13443 (2016) 1–12.
[24] The chemical structure of NLG919 analogue (7) is reported as NLG919 (GDC0919, 6) in the inhibitor catalog of selleckchem.com, 2014, page 117, Cat. No. S7111.
[25] S. Duhr, D. Braun, Why molecules move along a temperature gradient, Proc. Natl. Acad. Sci. U. S. A. 103 (2006) 19678–19682.
[26] C. Abad-Zapatero, Ligand efficiency indices for effective drug discovery, Expert Opin. Drug Discov. 2 (2007) 469–488.
[27] F. Fallarino, C. Uyttenhove, T. Boon, T.F. Gajewski, Endogenous IL-12 is necessary for rejection of P815 tumor variants in vivo, J. Immunol. 156 (1996) 1095–1100.
[28] Marvin 6.2.2, ChemAxon, 2014. http://www.chemaxon.com.